JOURNAL OF Materials CHEMISTRY

Synthesis and properties of a new series of mesogenic compounds with pyridine, oxidopyridinium, thienyl and furyl moieties†

Dorota Kardas,[a] Jozef Mieczkowski,[a] Damian Pociecha,*[b] Jadwiga Szydlowska[b] and Ewa Gorecka[b]

[a]*Laboratory of Chemistry of Natural Compounds, Department of Chemistry, Warsaw University, ul. Pasteura 1, 00–093 Warsaw, Poland*
[b]*Laboratory of Dielectrics and Magnetics, Department of Chemistry, Warsaw University, Al. Zwirki i Wigury 101, 02–089 Warsaw, Poland. Fax: +48 22 8221075; E-mail: pociu@chem.uw.edu.pl*

Received 30th August 2000, Accepted 27th November 2000
First published as an Advance Article on the web 11th January 2001

This paper presents the synthesis and mesophase properties of several homologous series of structurally related compounds in which the aromatic ring attached to 4′-alkyloxybiphenyl-4-ol was systematically changed. The homologues with achiral and chiral terminal groups were studied. New compounds forming both antiferroelectric and ferroelectric phases were obtained for pyridyl and phenyl derivatives.

Introduction

It is commonly believed that the type of molecular ordering in liquid crystal phases depends largely on the mesogenic core structure: its geometry, polarizability, molecular conformation, the length-to-breadth ratio as well as the number and position of permanent dipole moments in the core. In our previous works[1] it was shown that compounds with a biphenyl/phenyl core easily form tilted smectic phases in a broad temperature range. For these materials the synclinic or anticlinic[2] phases were observed, and the molecular tilt arrangement in neighbouring layers subtly depended on the length of the terminal chains attached to the mesogenic core. Here, we describe the synthesis and properties of related materials with a biphenyl/heterocycle (pyridine, oxidopyridinium, thienyl or furyl) core unit. The molecular structures of all compounds studied are presented in Table 1. The heterocyclic compounds have lower symmetry and different polarizability than the corresponding phenyl analogues. The heterocyclic compounds also possess an additional permanent dipole moment that affects the magnitude and direction of the total molecular dipole moment without increasing molecular breadth.

Experimental

The liquid crystalline phases were identified on the basis of routine examinations, namely by observation of created microscopic textures. For the texture observations a Nikon polarising microscope equipped with a METTLER FP82HT hot stage was used. The mesophase identification was supported by X-ray studies performed with a DRON diffractometer equipped with a graphite monochromator. For calorimetric measurements a DSC7 Perkin-Elmer set-up was used. Thermograms were recorded at a scanning rate of 5 K min^{-1}. The selective reflection wavelength was measured with a micro-spectrophotometry system based on the polarising microscope Nikon Optiphot2-Pol, working in the transmission mode. For compounds with long helical structure (order of microns) the helical pitch was estimated from the distance of dechiralization lines in thick (>50 μm) planar cells.[3]

The spontaneous polarisation was studied by the switching current method. The molecular tilt was measured as an angle difference between minimum transmission positions in the planar sample, which was placed under a microscope between crossed polarizers and subjected to opposite dc electric field. The identification of the polar properties of the phases was based mainly on observations of the apparent tilt and P_s electric switching.[2] In antiferroelectric phases the double current peak at spontaneous polarisation reversal and tristable electrooptic switching was detected in low frequency ($\sim$1 Hz) measurements. The ferroelectric–antiferroelectric phase transition was also monitored as a sudden change in the relative dielectric permittivity. Molecular dimensions were estimated by molecular modelling (HYPERCHEM 3.0).

In order to confirm the molecular structure of synthesised compounds some analytical methods were applied. Infrared (IR) spectra were obtained using a Nicolet Magna IR 500 spectrophotometer. NMR spectra were recorded on Varian Unity Plus Spectrophotometer operating at 500 MHz for ^{1}H NMR and at 125 MHz for ^{13}C NMR. Tetramethylsilane was used as an internal standard. Chemical shifts are reported in ppm. TLC analyses were performed on a Merck 60 silica gel glass plates and visualised using iodine vapour. The column chromatography was carried out at atmospheric pressure using silica gel (100–200 mesh, Merck).

Synthesis

Synthetic routes for the described compounds are outlined in Schemes 1–5. The pyridine derivatives, chiral and non-chiral (series **3**, **3a**, **4a** and compounds **3b, 3c, 3d, 3e**) were obtained according to the Schemes 2 and 3. The compound H (Scheme 3) was obtained according to the procedure described by Holland.[4] The synthesis of the compounds of the series **5** containing the oxidopyridinium ring proceeded according to Scheme 4. The compounds of the series **6**, **7**, **7a**, and **8** with thienyl or furyl rings were obtained following Scheme 5. The synthetic procedure giving the compounds of series **1** has been already described[1] and a similar procedure was applied to obtain the compounds of series **2** and **2a**.

†Elemental analyses for compounds in series **3**, **3a**, **3b**, **3c**, **3d**, **4a**, **5**, **6**, **7**, **7a** and **8** are available as supplementary data. For direct electronic access see http://www.rsc.org/suppdata/jm/b0/b007039o/

Table 1 Molecular structures of compounds studied

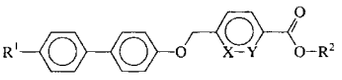

	X	Y	R^1	R^2
Series **1a**	CH	CH	OC_8H_{17}	$CH(CH_3)C_nH_{2n+1}$
Series **2**	CH	CH	$OC_{12}H_{25}$	C_nH_{2n+1}
Series **2a**	CH	CH	$OC_{12}H_{25}$	$CH(CH_3)C_nH_{2n+1}$
Series **3**	N	CH	$OC_{12}H_{25}$	C_nH_{2n+1}
Series **3a**	N	CH	$OC_{12}H_{25}$	$CH(CH_3)C_nH_{2n+1}$
Compound **3b**	N	CH	$OC_{12}H_{25}$	$CH_2CH(C_2H_5)C_4H_9$
	CH	N	$OC_{12}H_{25}$	CH_3
Compound **3c**	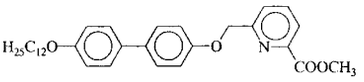			
Compound **3d**	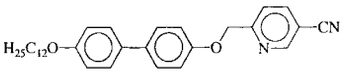			
Compound **3e**				
Series **4a**	N	CH	OC_8H_{17}	$CH(CH_3)C_nH_{2n+1}$
Series **5**	N→O	CH	$OC_{12}H_{25}$	C_nH_{2n+1}

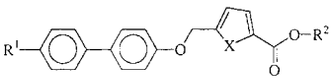

	X	R^1	R^2
Series **6**	S	OC_7H_{15}	C_nH_{2n+1}
Series **7**	S	$OC_{12}H_{25}$	C_nH_{2n+1}
Series **7a**	S	$OC_{12}H_{25}$	$CH(CH_3)C_nH_{2n+1}$

4-Hydroxy-4′-alkoxybiphenyl (B) (Scheme 1, reaction i). To 4,4′-dihydroxybiphenyl A (48 g, 260 mmol) in dimethylformamide (400 cm^3), dodecyl chloride (61 g, 300 mmol) and anhydrous potassium carbonate (40 g, 300 mmol) were added. The mixture was stirred and heated at 80 °C for 4 hours, then cooled to room temperature, and poured into water. The crude product was crystallised from methanol. The monoalkylated compound (B) (for $m=12$: 48 g, 53% yield) was obtained with sufficient purity for the next step.

In Schemes 2, 3 and 5 the Williamson reaction (ii) leading to related methyl esters was applied and as a model synthesis of methyl 5-(4′-alkoxybiphenyl-4-yloxymethyl)thiophene-2-carboxylate, which is the substrate of the series **6**, **7** and **7a**, is described.

Methyl 5-(4′-alkoxybiphenyl-4-yloxymethyl)thiophene-2-carboxylate. To 4-hydroxy-4′-alkoxybiphenyl (B) (for $m=12$: 3.5 g, 10 mmol) in dimethylformamide (25 cm^3) anhydrous potassium carbonate (2.1 g, 15 mmol) and methyl 5-(bromomethyl)thiophene-2-carboxylate (I) (2.7 g, 10 mmol) were added, stirred and heated at 35 °C for 3 days, cooled, poured into water and extracted six times with hot chloroform. The chloroform extracts were dried with anhydrous magnesium sulfate. The product was chromatographed on silica gel at an elevated temperature (40 °C) to avoid crystallisation and eluted with chloroform (for $m=12$: 3.5 g, 65% yield).

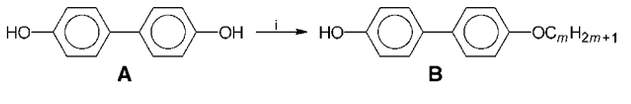

Scheme 1 *Reagents and conditions*: for reactions contained in Schemes 1–5: (i) $C_mH_{2m+1}Cl$(I), K_2CO_3, KI, DMF; (ii) B, K_2CO_3, DMF; (iii) KOH, C_4H_9OH, reflux; $(COCl)_2$, toluene, reflux; $HOCH^*(CH_3)C_nH_{2n+1}$, pyridine; (iv) $C_nH_{2n+1}OH$, H_2SO_4, toluene, reflux; (iva) $C_4H_9CH(C_2H_5)CH_2OH$, H_2SO_4, toluene, reflux; (v) NaH, Et_2O; (vi) $CNCH_2CONH_2$; (vii) PCl_5; (viii) Zn/AcOH; (ix) NBS, irradiation, reflux; (x) MCBA, CH_2Cl_2.

E.g.: Methyl 5-(4′-dodecyloxybiphenyl-4-yloxymethyl)thiophene-2-carboxylate

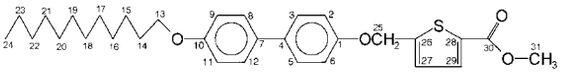

Elemental analysis for $C_{31}H_{40}O_4S$: Calc. C 73.19, H 7.93, S 6.30%; Found C 73.29, H 7.87, S 6.25%; ν_{max}(KBr)/cm^{-1}: 2940, 2830, 1610, 1500; ^{1}H NMR (δ; $CDCl_3$): 0.882 (t, 3H, CH_3(24), $J=7.0$ Hz), 1.2–1.5 (m, 18H, CH_2(15–24)), 1.729–1.880 (m, 2H, CH_2(14)), 3.908 (s, 2H, CH_3(31)), 3.984 (t, 2H, CH_2(13), $J=6.6$ Hz), 5.097 (s, 2H, CH_2(25)), 6.545 (d, 1H, H_{27}, $J_{27-28}=3.8$ Hz), 6.944 (dd, 2H, H_9H_{11}, $J_{9-8}=J_{11-12}=8.8$ Hz, $J_{9-11}=2.4$ Hz), 6.996 (d, 2H, H_2H_6, $J_{2-3}=J_{6-5}=8.8$ Hz, $J_{2-6}=2.4$ Hz), 7.175 (d, 1H, H_{27}, $J=3.4$ Hz), 7.456 (dd, 2H, H_8H_{12}, $J_{8-9}=J_{12-11}=8.8$ Hz, $J_{8-12}=2.4$ Hz), 7.475 (dd, 2H, H_3H_5, $J_{3-2}=J_{5-6}=8.8$ Hz, $J_{3-5}=2.4$ Hz), 7.707 (d, 1H, H_{28}, $J_{28-27}=4.0$ Hz); ^{13}C NMR (δ; $CDCl_3$): 14.13, 22.70, 26.08, 29.32, 29.36, 29.42, 29.61, 29.62, 29.65, 31.93, 52.21, 65.26, 68.12, 114.80, 115.25, 126.53, 127.66, 127.74, 127.82, 132.90, 133.38, 134.54, 147.10, 157.04, 158.24, 158.43.

The Williamson reaction was also used to obtain the compounds **3c**, **3d** and **3e** (Scheme 3).

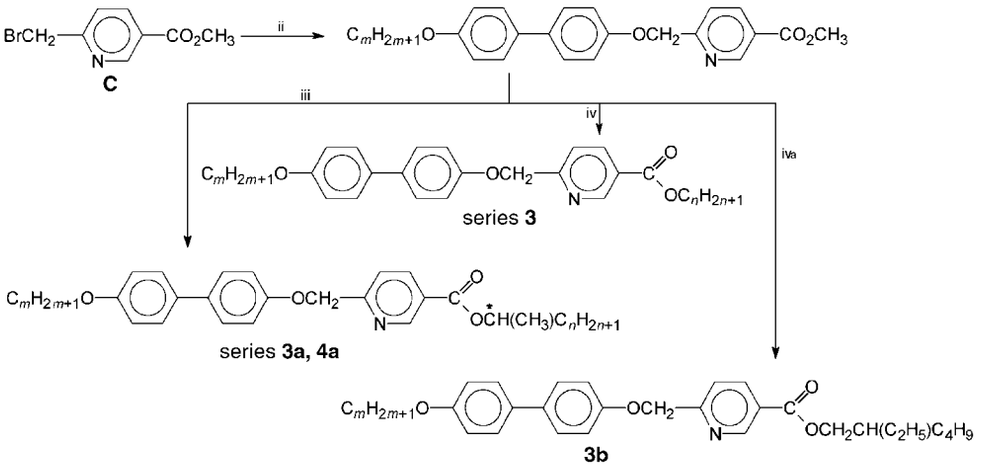

Scheme 2 For *reagents and conditions* see the legend to Scheme 1.

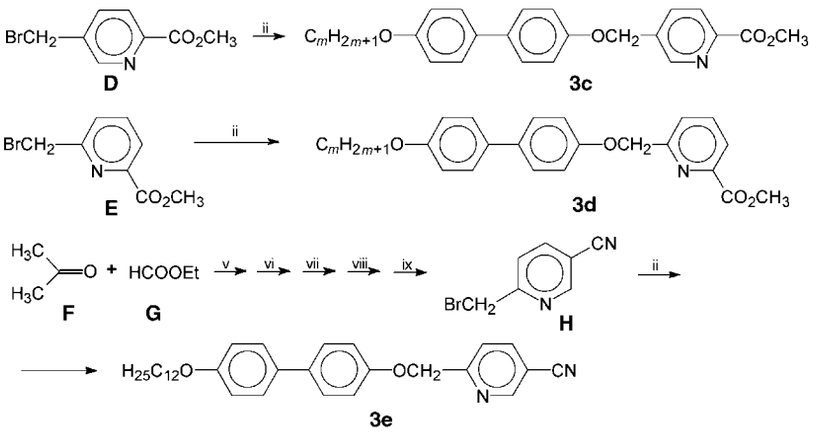

Scheme 3 For *reagents and conditions* see the legend to Scheme 1.

Preparation of pure enantiomeric series (Scheme 2 and 5, reaction iii). *Potassium salt.* The corresponding methyl ester (1 mmol) and potassium hydroxide (0.06 g, 1.5 mmol) in butanol (10 cm^3) were heated at reflux for 4 days. The product was filtered, washed with anhydrous ethyl ether and dried in a desiccator over phosphorous anhydride until the butanol smell disappeared. The potassium salt was obtained (yield varied from 85 to 90%).

E.g.: Potassium 5-(4′-dodecyloxybiphenyl-4-yloxymethyl)thiophene-2-carboxylate. Elemental analysis for $C_{30}H_{37}O_4SK$: Calc. C 67.63, H 7.00, S 6.02; Found C 67.65, H 7.05, S 6.00%; ν_{max}(KBr)/cm^{-1}: 2930, 2820, 1600, 1530, 1500, 1420, 1300. NMR measurements were not performed since these compounds form crystals which cannot be dissolved in standard solvents.

Optically active esters (series 3a, 4a, 7a). To the potassium salt (1 mmol) suspended in dry toluene (10 cm^3) oxalyl chloride (1.2 cm^3) was added and then the mixture was refluxed for two hours. The precipitated sodium chloride was filtered and the filtrate was evaporated to dryness. The acid chloride thus formed, dissolved in dry toluene (10 cm^3), was added to a mixture of the relevant alcohol (1 mmol) in pyridine (1 mmol). The reaction mixture was refluxed for 2 hours. Then, after evaporation of the solvents the product was purified with column chromatography on silica gel using toluene as eluent. Yields varied from 50 to 80%.

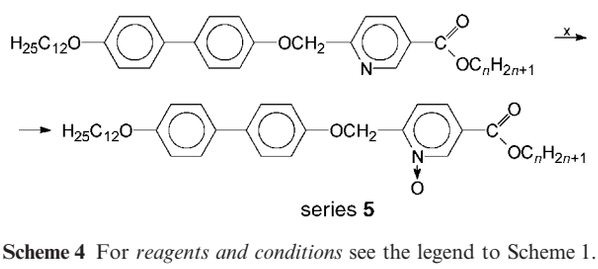

Scheme 4 For *reagents and conditions* see the legend to Scheme 1.

e.g.: (*R*)-(+)-2-Heptyl 5-(4′-dodecyloxybiphenyl-4-yloxymethyl)thiophene-2-carboxylate (series **7a**, $n=7$):

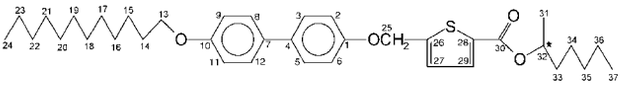

Elemental analysis for: $C_{37}H_{52}SO_4$: Calc.: C 74.96, H 8.86, S 5.41; Found: C 75.00, H 8.90, S 5.40%; ν_{max}(KBr)/cm^{-1}: 2980, 2950, 2900, 2850, 2800, 1710, 1600, 1500, 1280, 1250; ^{1}H NMR (δ; $CDCl_3$): 0.847 (t, 3H, CH_3(37), $J=6.5$ Hz), 0.880 (m, 3H, CH_3(24), $J=7.0$ Hz), 1.267–1.297 (m, 24H, CH_2(15–23, 34–36)), 1.312 (d, 3H, CH_3(31), $J=6.0$ Hz), 1.704–1.808 (m, 4H, CH_2(14, 33)), 3.968 (t, 2H, CH_2(13), $J=6.4$ Hz), 5.093 (sextet, 1H, CH(32), $J=6.2$ Hz), 5.223 (s, 2H, CH_2(25)), 6.934 (dd, 2H, H_9H_{11}, $J_{9-8}=J_{11-12}=8.8$ Hz, $J_{9-11}=2.2$ Hz), 6.996 (dd, 2H, H_2H_6, $J_{2-3}=J_{6-5}=8.8$ Hz, $J_{2-6}=4.5$ Hz), 7.066 (d, 1H, H_{27}, $J_{27-28}=3.8$ Hz), 7.448 (dd, 2H, H_8H_{12}, $J_{8-9}=J_{12-11}=8.8$ Hz, $J_{8-12}=2.4$ Hz), 7.480 (dd, 2H, H_3H_5, $J_{3-2}=J_{5-6}=8.8$ Hz, $J_{3-5}=4.5$ Hz), 7.680 (d, 1H, H_{28}, $J_{28-27}=3.8$ Hz); ^{13}C NMR (δ, $CDCl_3$): 12.98, 13.10, 19.03, 21.50, 21.68, 24.02, 25.04, 28.29, 28.34, 28.40, 28.59, 28.63, 30.59, 30.91, 34.91, 64.22, 67.05, 71.22, 113.73, 114.17, 125.45, 126.67, 126.73, 131.88, 133.40, 133.54, 134.56, 145.61, 156.05, 157.37, 160.76.

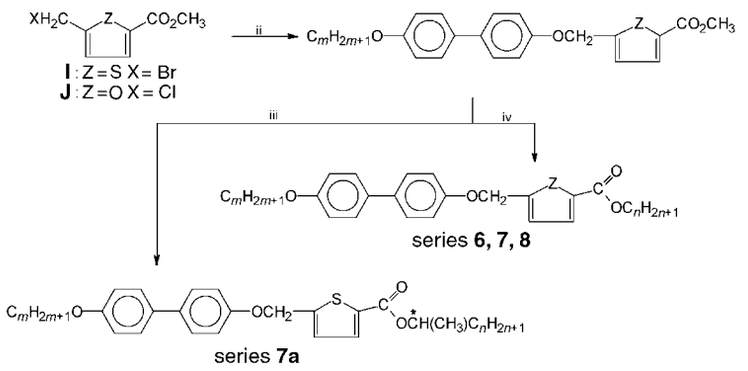

Scheme 5 For *reagents and conditions* see the legend to Scheme 1.

Achiral and racemic esters (series 3, 6, 7, 8 and compound 3b, Scheme 2 and 5, reaction iv and iva). To the appropriate methyl ester (0.25 mmol) a relevant achiral or racemic alcohol (5 cm^3) in toluene (20 cm^3) and concentrated sulfuric acid (4 drops) were added and heated for 5 hours under reflux. The reaction mixture was cooled, washed with 10% aqueous sodium carbonate and dried with magnesium sulfate. The product was chromatographed on silica gel using chloroform as eluent. Yields varied from 80 to 95%.

e.g. Butyl 5-(4′-dodecyloxybiphenyl-4-yloxymethyl)furan-2-carboxylate (series **8**, $n=4$)

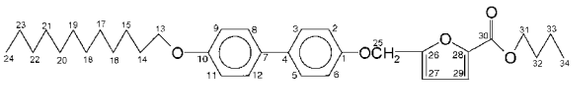

Elemental analysis for: $C_{34}H_{46}O_5$: Calc.: C 76.37, H 8.67; Found: C 76.40, H 8.70%; ν_{max}(KBr)/cm^{-1}: 2980, 2950, 2900, 2850, 2800, 1710, 1600, 1500, 1280, 1250; ^{1}H NMR (δ; $CDCl_3$): 0.882 (t, 3H, CH_3(24), $J=6.0$ Hz), 0.967 (t, 3H, CH_3(34), $J=6.8$ Hz), 1.267–1.502 (m, 20H, CH_2(15–23, 33)), 1.663–1.832 (m, 4H, CH_2(14, 32)), 3.981 (t, 2H, CH_2(13), $J=6.8$ Hz), 4.315 (t, 2H, CH_2(31), $J=6.8$ Hz), 5.092(s, 2H, CH_2(25)), 6.533 (d, 1H, H_{27}, $J_{27-28}=3.4$ Hz), 6.943 (dd, 2H, H_9H_{11}, $J_{9-11}=2.2$ Hz, $J_{9-8}=J_{11-12}=8.8$ Hz), 6.999 (d, 2H, H_2H_6, $J_{2-6}=2.2$ Hz, $J_{2-3}=J_{6-5}=8.8$ Hz), 7.174 (d, 1H, H_{28}, $J_{28-27}=3.4$ Hz), 7.456 (dd, 2H, H_8H_{12}, $J_{8-12}=2.2$ Hz, $J_{8-9}=J_{12-11}=8.8$ Hz), 7.473 (dd, 2H, H_3H_5, $J_{3-5}=2.2$ Hz, $J_{3-2}=J_{5-6}=8.8$ Hz); ^{13}C NMR (δ; $CDCl_3$): 13.70, 14.10, 19.10, 22.67, 26.03, 29.27, 29.33, 29.39, 29.56, 29.59, 29.61, 29.64, 30.69, 31.89, 51.99, 62.56, 64.88, 68.06, 107.01, 111.23, 114.73, 115.03, 118.52, 127.67, 127.72, 132.94, 134.37, 144.73, 157.04, 158.34, 159.05.

Esters of 6-(4′-dodecyloxybiphenyl-4-yloxymethyl)-3-(alkoxycarbonyl)pyridinium-1-olate (series 5). To the relevant ester of the series **3** (0.2 mmol) which was dissolved in methylene chloride (10 cm^3), MCBA (0.3 mmol) was added, stirred for 5 days in room temperature. After evaporation of the solvent the product was purified with column chromatography on silica gel using chloroform as eluent. Yields varied from 80 to 95%.

e.g.: 6-(4′-Dodecyloxybiphenyl-4-yloxymethyl)-3-(butyloxycarbonyl)pyridinium-1-olate (series **5**, $n=4$)

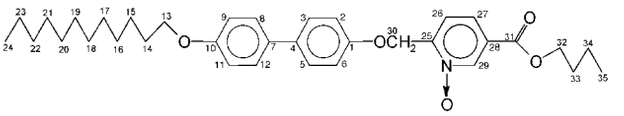

Elemental analysis for: $C_{35}H_{47}NO_5$: Calc.: C 74.84, H 8.43, N 2.49; Found: C 74.80, H 8.40, N 2.50%; ν_{max}(KBr)/cm^{-1}: 2990, 2960, 2910, 2850, 2810, 1730, 1610, 1500, 1280, 1250; ^{1}H NMR (δ; $CDCl_3$): 0.882 (t, 3H, CH_3(24), $J=6.4$ Hz), 0.984 (t, 3H, CH_3(35), $J=6.4$ Hz), 1.267–1.485 (m, 20H, CH_2(15–23, 34)), 1.755 (quintet, 2H, CH_2(14), $J=6.4$ Hz), 1.761 (quintet, 2H, CH_2(33), $J=6.4$ Hz), 3.983 (t, 2H, CH_2(13), $J=6.4$ Hz), 4.369 (t, 2H, CH_2(32), $J=6.4$ Hz), 5.382 (s, 2H, CH_2(30)), 6.948 (dd, 2H, H_9H_{11}, $J_{9-11}=2.4$ Hz, $J_{9-8}=J_{11-12}=8.8$ Hz), 7.065 (dd, 2H, H_2H_6, $J_{2-6}=2.4$ Hz, $J_{2-3}=J_{6-5}=8.8$ Hz), 7.463 (dd, 2H, H_8H_{12}, $J_{8-12}=2.4$ Hz, $J_{8-9}=J_{12-11}=8.8$ Hz), 7.504 (dd, 2H, H_3H_5, $J_{3-5}=2.4$ Hz, $J_{3-2}=J_{5-6}=8.8$ Hz), 7.736 (d, 1H, H_{26}, $J_{26-27}=8.4$ Hz), 7.917 (dd, 1H, H_{27}, $J_{27-29}=2.2$ Hz, $J_{27-26}=8.4$ Hz), 8.865 (d, 1H, H_{29}, $J_{29-27}=2.2$ Hz); ^{13}C NMR (δ; $CDCl_3$): 13.65, 14.09, 19.14, 22.67, 26.04, 29.24, 29.32, 29.38, 29.42, 29.58, 29.65, 30.51, 31.89, 35.70, 64.35, 66.04, 68.09, 114.77, 114.89, 123.22, 126.25, 127.70, 127.93, 132.76, 134.79, 140.11, 152.01, 156.56, 158.45, 162.97, 164.32.

Results and discussion

The measured phase transition temperatures and enthalpy changes are collected in Tables 2–12. The data for comparative phenyl compounds (series **1a**) with a chiral ester tail attached to the phenyl unit are presented in ref. 1. Phase diagrams for chiral series **2a**, **3a**, **4a** and **7a** are shown inFig. 1. For simplicity, we divided our considerations into two parts: one related to the pyridine and oxidopyridinium derivatives (six-membered hetero-rings), and the other describing the thiophene and furan series (five-membered hetero-rings). For each homologous series the length of the *n*-alkyl tail at the biphenyl moiety was fixed (usually 12 or 8 carbon atoms), while the

Table 2 Phase transition temperatures (°C) and, in parentheses, their thermal effects (kJ mol^{-1}) for the compounds of series **2**

n	Mp	CryX		CryJ		SmI		SmC		CryE		CryB		SmA		Iso
1	136.3 (44.19)									•	172.9 (3.68)	•	198.6 (3.47)	•	204.4 (18.28)	•
4	89 (44.55)	•	123.7 (2.27)	•	124.6 (0.03)	•	152.8 (4.22)	•	166.6 (0.18)					•	169.9 (16.05)	•
8	94.3 (49.55)	•	117.2 (2.84)	•	120.7 (0.08)	•	142.1 (3.47)	•	158.4 (19.16)							•

Table 3 Phase transition temperatures (°C) and, in parentheses, their thermal effects (kJ mol^{-1}) for the compounds of series **2a**

n	Mp	CryJ		SmI*$_A$		SmI*		SmC*$_A$		SmC*		Iso
2	74.8 (8.54)	•	101.8 (1.69)			•	133.4 (2.33)			•	150.2 (13.56)	•
3	77.4 (31.16)	•	92.3 (1.46)			•	116.1 (1.07)			•	136.6 (13.10)	•
4	76.5 (34.35)	•	89.1 (1.40)	•	110.4 (1.42)			•	125.0 (0.03)	•	133.2 (13.07)	•
5	86.0 (41.60)	•	88.0 (1.58)			•	106.5 (1.65)			•	127.1 (13.66)	•
6	81.2 (31.23)	•	89.5 (4.87)	•	104.0 (2.02)			•	119.3 (0.05)	•	123.6 (13.56)	•

Table 4 Phase transition temperatures (°C) and, in parentheses, their thermal effects (kJ mol^{-1}) for the compounds of series **3**

n	Mp	CryJ		CryX		SmI		SmC		SmA		Iso
1	175.2 (46.39)									•	187.3 (17.56)	•
2	131.8 (40.87)	•	128.4 (4.23)			•	141.4 (2.36)	•		•	169.20 (17.11)	•
4	113.4 (37.83)	•	109.8 (3.74)	•	110.8 (0.03)	•	125.1 (2.07)	•	153.8 (16.01)			•
8	113.4 (36.85)	•	107.2 (3.37)			•	119.6 (1.4)	•	150.2 (16.40)			•

Table 5 Phase transition temperatures (°C) and, in parentheses, their thermal effects (kJ mol^{-1}) for the compounds of series **3a**

n	Mp	CryJ		SmI*$_A$		SmI*		SmC*$_A$		SmC*		Iso
2	95.4 (36.90)					•	106.7 (2.17)			•	133.2 (13.92)	•
3	99.7 (47.95)			•	95.6 (0.78)			•	118.36 (0.02)	•	121.9 (13.30)	•
4	95.3 (44.92)	•	80.0 (0.69)	•	87.7 (0.75)			•	115[a]	•	117.2 (13.52)	•
5	106.3 (52.25)									•	114.4 (14.02)	•
6	106.3 (48.85)							•	103.5[a]	•	111.3 (13.58)	•

[a]From microscopic and dielectric studies.

length of the tail attached to the heterocycle moiety was systematically varied.

Pyridine and oxidopyridinium series

Compounds of the series **3** with the pyridine moiety substituted at the 3 position by an *n*-alkyl ester group exhibit typical mesophase polymorphism. For the shortest homologues ($n=1$, 2) the orthogonal SmA phase is observed whereas extension of the alkyl chain results in a sequence of tilted smectic phases. It should be noticed that the introduction of the pyridyl ring into the core structure instead of the phenyl ring makes the orthogonal mesophases less ordered. For the analogous phenyl derivatives (series **2**) soft crystalline phases (CryB, CryE) appear and exist in the broad temperature range. The clearing temperatures for compounds of series **2** are about 10 K higher and melting temperatures about 20 K lower than for compounds of series **3** with the same molecular length. Moreover, the difference in the layer spacing in the tilted phases was observed between relevant homologues of series **3** and **2**, and higher tilt angles for pyridine compounds were observed. At the SmC–hexatic SmI phase transition, a continuous increase of the in-plane molecular density and dilatation of the smectic layer thickness were detected and this suggests the overcritical nature of the changes of the phase structure.[5] For oxidopyridinium derivatives (series **5**) the clearing temperatures coincide with the clearing temperatures of the pyridine derivatives, and only slightly higher melting temperatures were found. These compounds, however, have a much stronger tendency to re-

Table 6 Phase transition temperatures (°C) and, in parentheses, their thermal effects (kJ mol^{-1}) for the compounds **3b**–**3e**

Compound	Mp	SmC		SmA		Iso
3b	87.5 (27.48)	•	109.8 (8.62)			•
3c	161.5 (38.05)			•	211.0 (6.87)	•
3d	137.0 (44.86)					•
3e	138.3 (40.29)			•[a]	173.4 (9.77)	•

[a]SmA_d.

crystallise thus no monotropic mesophases could be observed below the SmC phase. The layer spacing in the SmC phase formed by the compounds of series **5** was slightly smaller ($\sim$0.5 Å) than for the corresponding non-oxidised compounds (Fig. 2). For material with a CN group attached to the pyridine ring (compound **3e**) the partial bilayer ($d/L\sim1.4$) smectic A_d phase[6] is observed. The pyridine derivative in which the terminal chain is moved to a lateral position (compound **3d**) does not form liquid crystalline phases. Placing the nitrogen atom of the pyridine moiety at a position closer to the terminal chain (compound **3c**) does not change the mesophase sequence. However, the liquid crystalline stability range increases: the melting temperature is $\sim$15 K lower and the clearing temperature $\sim$30 K higher than for the corresponding compound of series **3**.

The phenyl (series **2a**) as well as the pyridyl (series **3a** and **4a**) derivatives with an asymmetric carbon atom in the terminal chain were also examined. Their clearing and melting temperatures are visibly depressed compared with the non-branched terminal-chain compounds (series **2** and **3**). For phenyl homologues of series **2a** with $n=2$, 3, 5 ferroelectric phases are exclusively observed, the other two studied compounds with chiral chain length $n=4$, 6 show also antiferroelectric phases (SmI*$_A$ and SmC*$_A$) stable over a broad temperature range below the short ferroelectric SmC* phase. Exchange of the phenyl ring (series **2a**) with the pyridyl ring (series **3a**) increases the ability to form antiferroelectric phases, the anticlinic structure is formed by three homologues $n=3$, 4, 6. The spontaneous polarisation (Fig. 3) for the pyridyl derivatives (up to 100 nC cm^{-2} for compounds of series **3a** and less than 50 nC cm^{-2} for compounds of series **4a**) is significantly lower than for phenyl derivatives (up to 270 nC cm^{-2}) in series **2a**. As the tilt in the SmC* and SmC*$_A$ phases of the pyridyl and phenyl derivatives is similar ($\sim$35°) the changes of P_s have to be related to the changes in the transverse dipole moment of molecules. In the pyridyl series **4a** in which the non-chiral tail is cut off to 8 carbon atoms the non-tilted phases (CryB and CryE) were observed starting from $n>2$. For this series a interesting re-entrant phenomenon was

Table 7 Phase transition temperatures (°C) and, in parentheses, their thermal effects (kJ mol^{-1}) for the compounds of series **4a**

n	Mp	CryE		CryB		CryJ		SmI*		SmC^*_{re}		SmC^*_A		SmC*		Iso
2	112.0 (11.45)					•	111.6 (3.42)	•	126.7 (2.32)	•	128.2 (0.01)	•	142[a]	•	142.5 (13.83)	•
3	81.7 (18.42)	•	105.3 (3.08)	•	120.86[b]			•	121.7[b]	•	122.4[b]	•	132[a]	•	133.1 (14.41)	•
4	84.3 (23.42)	•	95.6 (3.02)	•	118.6 (3.12)					•	119.3 (0.03)	•	126.6 (0.02)	•	129.4 (14.01)	•
5	98.4 (35.32)	•	96.5 (3.28)	•	117.6 (3.44)									•	125.2 (14.21)	•
6	97.0 (34.10)	•	95.7 (3.38)	•	115.0 (3.42)									•	122.3 (13.91)	•

[a]From microscopic and dielectric studies. [b]Signals not resolved, total enthalpy changes 2.84 [kJ mol^{-1}].

Table 8 Phase transition temperatures (°C) and, in parentheses, their thermal effects (kJ mol^{-1}) for the compounds of series **5**

n	Mp	SmC		Iso
4	125.6 (41.00)	•	153.4 (10.50)	•
8	128.5 (33.30)	•	148.0 (14.12)	•

Table 9 Phase transition temperatures (°C) and, in parentheses, their thermal effects (kJ mol^{-1}) for the compounds of series **6**

n	Mp	SmA		Iso
1	134.5 (37.35)	•	165.9 (8.00)	•
4	134.8 (22.67)	•	166.2 (8.75)	•
8	129.5 (46.12)	•	165.1 (9.71)	•

Table 10 Phase transition temperatures (°C) and, in parentheses, their thermal effects (kJ mol^{-1}) for the compounds of series **7**

n	Mp	CryJ		SmI		SmC		SmA		Iso
1	147.0 (25.44)							•	146 (11.28)	•
4	94.5 (40.70)	•	88.3 (2.09)	•	114.6 (1.76)	•	133.3 (12.74)			•
8	84.9 (38.66)	•	85.7 (4.93)	•	105.6 (2.24)	•	122.8 (16.39)			•

Table 11 Phase transition temperatures (°C) and, in parentheses, their thermal effects (kJ mol^{-1}) for the compounds of series **7a**

n	Mp	CryJ		SmI*		SmC*		Iso
2	<50	•	76.3 (1.46)	•	96.5 (1.24)	•	114.0 (12.26)	•
3	61.4 (31.08)	•	68.9 (1.49)	•	81.4 (0.67)	•	105.1 (11.66)	•
4	55.6 (31.41)	•	67.2 (1.93)	•	73.8 (0.52)	•	98.2 (10.98)	•
5	64.5 (19.61)	•	67.0 (2.06)	•	71.5 (0.50)	•	101.4 (14.25)	•
6	64.7 (38.53)	•	60.5 (2.40)	•	69.4 (0.48)	•	93.3 (12.08)	•

Table 12 Phase transition temperatures (°C), taken from microscopic studies, for the compounds of series **8**

n	Mp	CryB		SmC		SmA		Iso
1	120							•
4	99.4	•	100			•	102	•
8	81.0			•	99	•	103	•

detected, for homologues with $n=2$, 3, 4 ferroelectric properties re-appear (SmC* and SmI*) below the antiferroelectric SmC^*_A phase. For homologues $n=2$, 3 phase sequence Iso–SmC*–SmC^*_A–SmC*–SmI* and for $n=4$ Iso–SmC*–SmC^*_A–SmC*–CryB was found. In all three studied chiral series (**2a**, **3a**, **4a**) the ferroelectric SmC* phase exhibits a rather short helioelectric structure. For compounds of the pyridyl **3a** and the phenyl **2a** series the selective reflection was observed in the visible range, except for the shortest homologues. Within a homologue series, the helical pitch decreases with increasing length of the chiral tail. It is ~650 nm, 500 nm, 400 nm for homologues of series **3a** with $n=3$, 4, 6, respectively, when measured in the temperature range 1–2 K below the clearing point. For the corresponding homologues of the phenyl series the selective reflection is shifted toward a longer wavelength range (*e.g.* 650 nm for homologue $n=4$ of series **2a**). For both series in the smectic C* phase as the temperature decreases, the helix pitch shortens, it varies smoothly through the SmC*–SmI* phase transition. If the material exhibits antiferroelectric phases the sense of the helix changes at the SmC*–SmC^*_A phase transition and in the SmC^*_A phase the temperature dependence for the helix pitch is reversed to that observed in the SmC* phase. Below SmC*–SmC^*_A phase transition the helix pitch is in the μm range, as the temperature is lowered the helix unwinds. The helix becomes infinitive ~10–20 K below the SmC*–SmC^*_A phase transition, this is signified by the appearance of a stripe or square texture in the free suspended thick (>10 μm) films[7] and a schlieren texture in the homeotropically aligned thin samples placed between glasses.

The oxidopyridinium chiral derivatives were also obtained, however attempts to purify them failed, thus their physical properties were not studied.

Series with five-membered heterocyclic rings

For all the series with thienyl (**6** and **7**) and furyl (**8**), with *n*-alkyl terminal chains the phase sequences are similar, short homologues form non-tilted phases while longer ones exhibit also tilted phases. The clearing temperatures for compounds of the series with five-membered heterocyclic rings are lower than for the corresponding materials of series with six-membered rings, this is typical as the five-atom ring in the core slightly bends the molecular structure. The mesophase stability of the thienyl derivatives is evidently higher than of furyl derivatives, as the bending imposed by the furyl ring is stronger than the one caused by the thienyl moiety.[8] The core bending is also responsible for shorter layer spacing observed for thienyl compounds compared with pyridyl ones (Fig. 4). The derivatives with branched chiral chains attached to the thienyl ring (series **7a**) form exclusively ferroelectric phases, SmC*, SmI* and CryJ phase. Both SmC* and SmI* phases have a helioelectric structure with a helical pitch of a few μm and this does not change significantly at the SmC*–SmI* phase transition. The electric spontaneous polarisation (up to 170 nC cm^{-2}) is lower than for phenyl derivatives (series **2a**), but slightly higher than that observed for the pyridyl series **3a**.

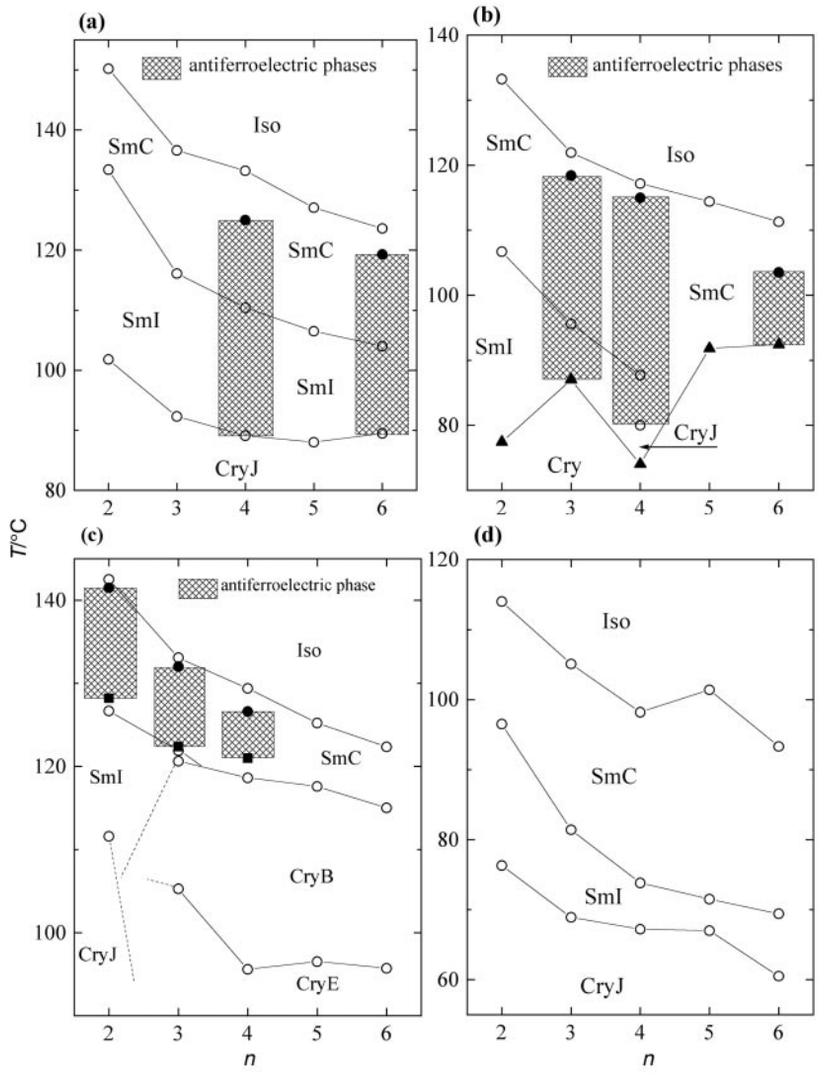

Fig. 1 Phase diagrams for (a) homologous series **2a**, (b) series **3a**, (c) series **4a** and (d) series **7a**; the length of the chiral tail, *n*, is changed.

Summary

The six-membered heterocyclic compounds with achiral as well as chiral ester chains generally melt higher than their phenyl analogues and their clearing temperatures are lower. For the series with five-membered heterocycles both the clearing and melting temperatures are decreased. For these compounds a disturbed rod-like shape imposed by the five-membered ring is an important factor in lowering the thermal stability of mesophases and crystalline phases.

Comparison of the properties of chiral pyridyl and thienyl compounds with their phenyl analogues shows that the presence of a heteroatom influences significantly the magnitude of spontaneous polarisation and the length of the helical pitch. The P_s value depends greatly on the dipole moments, rotation of which could be biased by the presence of the chiral centre, *e.g.* on the ester group dipole.[9] The presence of a heterocycle with electron-accepting properties can affect the value of

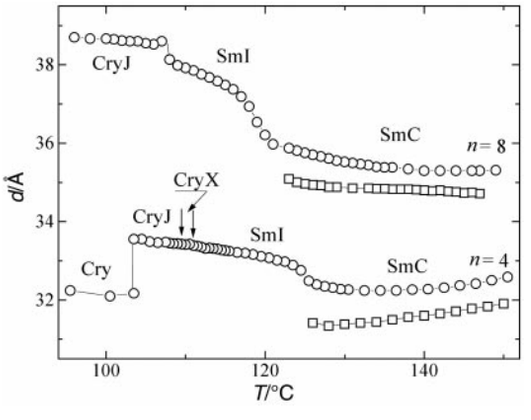

Fig. 2 Temperature dependence of the smectic layer thickness for homologues $n=4$ and $n=8$ of series **3** (circles) and **5** (squares).

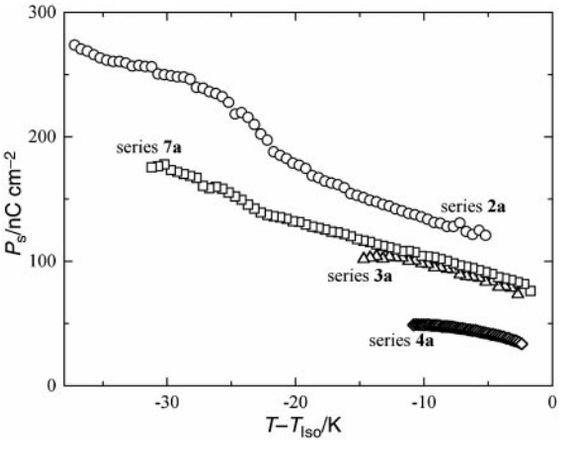

Fig. 3 Temperature dependence of the spontaneous polarisation for homologues $n=4$ of the series **2a**, **3a**, **4a** and **7a**.

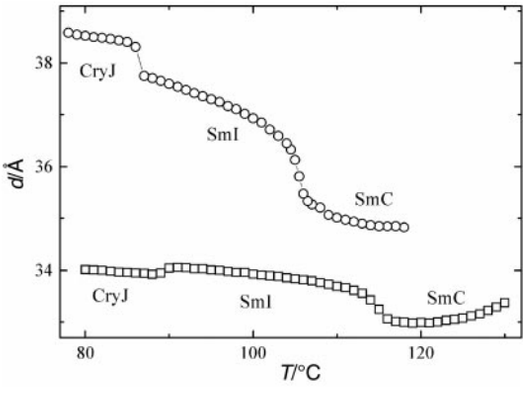

Fig. 4 Temperature dependence of the smectic layer thickness for homologues $n=4$ (squares) and $n=8$ (circles) of series **7**.

spontaneous polarisation by lowering the electron density of the ester group and thus decreasing its dipole moment. The possibility that the dipole moment of the heterocyclic ring and the dipole moment of the terminal chain are partially compensated should be ruled out, since this would require strongly biased rotation of the core with respect to the molecular tail. An observed increase of twisting power in homologous series (*e.g.* series **2a**, **3a**), as indicated by the decrease of the helical pitch with the increase of the chiral tail length seems to be caused by increased rotation restrictions of the longer groups attached to the chiral centre.

For the materials with pyridyl and phenyl ring in the mesogenic core the anticlinic tilted phases (antiferroelectric) could be observed. It seems that changes in the polarizability of the core induced by replacement of the phenyl ring with a pyridyl ring did not influence significantly the stability of the anticlinic or synclinic structure. For both groups of compounds the energy of the anticlinic and synclinic interactions must be very similar, and the type of the tilt structure between neighbouring layers is determined mainly by such factors as the geometry of tails and degree of their interdigitation between the layers. On the other hand, for the thienyl derivative only ferroelectric SmC* and SmI* phases are observed, which shows that bending of the molecule core imposed by the five-membered ring makes the synclinic structure more favourable, and the phase sequence less sensitive to the tail's geometry.

Acknowledgements

Authors would like to thank Professor Jan Przedmojski from Warsaw University of Technology for providing us with X-ray facilities and his help with the measurements. The work was supported by KBN Grant 3 T09A 04615 and synthesis by 3 T09A 09519.

References

1 J. Szydlowska, D. Pociecha, E. Gorecka, D. Kardas, J. Mieczkowski and J. Przedmojski, *J. Mater. Chem.*, 1999, **9**, 361.
2 A. D. L. Chandani, E. Gorecka, Y. Ouchi, H. Takezoe and A. Fukuda, *Jap. J. Appl. Phys.*, 1990, **29**, 131.
3 M. Brunet and C. Williams, *Ann. Phys. (Paris)*, 1978, **3**, 137; M. Glogarova, L. Lejcek, J. Pavel, U. Janovec and F. Fousek, *Mol. Cryst. Liq. Cryst.*, 1983, **91**, 309.
4 G. F. Holland and J. N. Pereira, *J. Med. Chem.*, 1967, **10**, 149–154.
5 S. K. Prasad, D. S. Shankar Rao, S. Chandrasekhar, M. Neubert and J. Goodby, *Phys. Rev. Lett.*, 1995, **74**, 270; S. K. Prasad, G. Nair and S. Chandrasekhar, *J. Mater. Chem.*, 1995, **5**, 2253.
6 S. Chandrasekhar, in *Liquid Crystals*, Cambridge University Press, Cambridge, 1992, p. 350.
7 E. Gorecka, M. Glogarova, L. Lejcek and H. Sverenyak, *Phys. Rev. Lett.*, 1995, **75**, 4047.
8 J. Szydlowska, D. Pociecha, A. Krowczynski and E. Gorecka, *Mol. Cryst. Liq. Cryst.*, 1997, **301**, 19.
9 A. Terzis, D. Photinos and E. Samulski, *J. Chem. Phys.*, 1997, **107**, 4061.